Photocatalytic degradation of geosmin:
Reaction pathway analysis

Emomotimi E Bamuza-Pemu and Evans MN Chirwa*

Water Utilisation Division, University of Pretoria, Pretoria, 0002, South Africa

Abstract

The presence of geosmin in drinking water imparts a musty odour which leads to consumer complaints. Geosmin and other unwanted organics can be treated using photocatalysis. However, the intermediates formed during the photocatalytic degradation process and their degradation pathways have not previously been described. In this study, the degradation profile, as well as the intermediates formed during the photocatalytic degradation of geosmin was monitored in an effort to obtain a better understanding of the degradation kinetics and pathway. Photocatalytic degradation of geosmin in the presence of radical scavengers was shown to be inhibited, as evidenced by the reduction in reaction rate coefficient (k') from 0.055 to 0.038 min^{-1}. The hydroxyl radical reaction was thus shown to be the predominant process over direct photolysis by incident UV energy. Results from mass spectrum analysis of degradation intermediates indicate rapid fission of sp^3—sp^3 (C—C) bonds resulting in ring opening of the cyclic geosmin structure. Bicyclic compounds that could be expected from dehydration and dehydrogenation of geosmin's ringed structure were not found among the detected intermediate products. Intermediates identified consisted of acyclic unsaturated alkenes, carbonyl compounds and some organic acids. Although the identified degradation products are not seen to be directly harmful, chlorine disinfection of water containing these compounds could produce potentially harmful halogenated hydrocarbons.

Keywords: photocatalysis, geosmin, 2-methylisoborneol (2-MIB), taste and odour, degradation intermediates

Introduction

Producing drinking water of good aesthetic quality is a major goal for all water authorities, mainly because consumers will judge suitability of the water based on its tactile quality (i.e., clarity, smell and taste). Although description of water as aesthetically-poor does not necessarily imply that the water is unsafe for consumption, it does indicate that there may be a problem with the treatment process (Nerenberg et al., 2000; Ho and Newcombe, 2010). Furthermore, good chemical quality is important beyond the water's aesthetic quality. This is because, at the present time, the majority of water resources – both surface water and groundwater – have been polluted with a variety of toxic and carcinogenic organic pollutants received from untreated or partially-treated domestic and industrial wastewaters and agricultural run-off (Griffini et al., 1999). Furthermore, large nutrient inputs from the above pollution sources have been associated with algal and cyanobacterial blooms in surface water bodies, which in turn result in the production of toxic organics and taste- and nuisance-causing compounds.

In this study, the feasibility of treating common algal metabolites, such as geosmin (trans-1,10-dimethyl-trans-9-decalol) and 2-MIB (2-methylisoborneol), using a photocatalytic process is evaluated. Geosmin and 2-MIB impart taste and odour to water, thereby compromising the aesthetic quality of the water (Peter and Von Gunten, 2007). The presence of these compounds also causes undesirable taint problems in the aquaculture industry. Geosmin and 2-MIB are bicyclic tertiary alcohols produced as secondary metabolites of blue-green algae (cyanobacteria), and are also known as actinomycetes (Tran et al., 2008; Watson et al., 2003). Geosmin is also produced by *Streptomyces* and myxobacteria and is responsible for the characteristic odour of freshly-turned earth (Cane et al., 2006). Some soil bacteria are also known to produce geosmin. The soil bacteria may be washed by rainfall runoff into nearby streams where they further increase the prevalence of odour-causing compounds in surface waters.

The odour detection threshold in humans has been reported at concentrations as low as 1.3 ng·ℓ^{-1} for geosmin and 6.3 ng·ℓ^{-1} for 2-MIB (Young et al., 1996; Lloyd et al., 1998). Due to the low human detection threshold, effective treatment of the taste and odour compounds to levels below the human detection threshold is a major challenge to the water industry. So far, a variety of physical-chemical treatment technologies, such as oxidation by ozonation, adsorption on granular activated carbon (GAC) or powder activated carbon (PAC) particles, and biodegradation in biofilters, have been employed in treating taste- and odour-causing compounds. However, almost all of these technologies have been found lacking, either due to poor treatment efficiency or due to high capital and operational costs. For example, relatively low performance (as low as 69%) was achievable in GAC adsorption applied for removing compounds with molecular structures similar to geosmin (Pham et al., 2012).

Over the past three decades, advances in research have yielded novel applications, such as advanced oxidation processes (AOPs) which utilise the oxidative power of the hydroxyl radicals to mineralise organics in water. AOPs have been acclaimed for their ability to completely mineralise organic compounds to CO_2 and H_2O, and are therefore categorised as clean technologies (Chirwa and Bamuza-Pemu, 2010; Tran et al., 2009; Lawton et al., 2003). In studies by

---

* To whom all correspondence should be addressed.
☎ +27 12 420 5894; fax: +27 12 362 5089;
e-mail: Evans.Chirwa@up.ac.za

Received 25 July 2011; accepted in revised form 1 October 2012.

Chirwa and Bamuza-Pemu (2010), geosmin was effectively removed in water at catalyst concentrations ranging from 50 to 60 mg $TiO_2 \cdot \ell^{-1}$. In the above study, complete degradation was observed in batches at initial geosmin concentrations up to 220 ng$\cdot\ell^{-1}$, in less than 60 min. Further investigations showed that the presence of hydroxyl radical scavengers such as sodium bicarbonate, and tertiary butanol (t-BuOH) reduced the overall geosmin degradation.

Other clean technologies, such as ultrasonic cavitation with pyrolytic bond cleavage, have also been considered for treatment of toxic organics and taste- and odour-causing compounds in water (Song and O'Shea, 2007). However, the feasibility of cavitation and pyrolytic systems for treating large streams typically encountered in water treatment plants has not been demonstrated to date.

This study elucidates the mode of degradation of geosmin around catalyst particles using a mathematical modelling approach. Although studies on photocatalytic degradation are commonly available in literature, none of these studies attempted to investigate the pathway involved and the occurrence of potentially harmful intermediates formed during the degradation process. This study aimed to show both the trend and sequence of events during the degradation of geosmin.
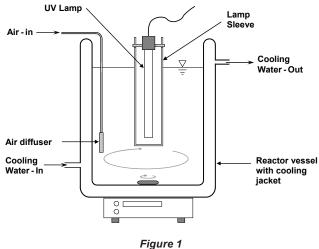
Experimental procedure

Chemicals

Geosmin was purchased as an analytical standard solution of 100 mg$\cdot\ell^{-1}$ in methanol, from Sigma-Aldrich, Germany. Tertiary butanol was obtained from Merck, South Africa. All solutions were prepared using ultrapure water from Milli-Q, Millipore Direct Q_3 (supplied by Microsep, Johannesburg, South Africa).

Materials

The UV radiation source used in this study consisted of an artificial long-arc 400 W medium pressure lamp (Philips, Netherlands, supplied by Technilamps, South Africa). UV radiation intensity in reactors was measured with Goldilux UV Smartmeters, Model GRP-1 (USA, supplied by MIT, South Africa). The meters were calibrated at the National Metrology Institute of South Africa (NMISA). The UV lamp's radiance intensity (33.65 mW$\cdot$cm^{-2}) produced a spectral output with an overlapping wavelength range and maximum wavelength, λ_{max} = 365 nm. Anatase TiO_2 powder (99.8% pure) was purchased from Sigma-Aldrich, Germany and used as received. Progress of geosmin degradation was monitored chromatographically as described under 'Analysis' (below).

Degradation studies

Photocatalytic degradation of geosmin was conducted in batch systems with 1 ℓ solutions at initial concentrations of 220 ng$\cdot\ell^{-1}$, 500 ng$\cdot\ell^{-1}$ and 10 μg$\cdot\ell^{-1}$. Geosmin solutions were prepared by spiking ultrapure water with the appropriate quantities of geosmin standards. The solutions were irradiated with a medium pressure 400 W UV lamp in the absence of TiO_2 (photolytic degradation) and in the presence of 40 mg$\cdot\ell^{-1}$ anatase TiO_2. Photocatalytic degradation of geosmin was also conducted in the presence of a radical scavenger, 0.1 mol$\cdot\ell^{-1}$ tertiary butanol (t-BuOH), to evaluate the extent of photolysis and surface

Figure 1
Photocatalytic reactor setup showing lamp housing and cooling system

catalysis on TiO_2 particles. The UV lamp was housed in a double-walled quartz sleeve which provided a channel for cooling of the lamp and reactor contents (Fig. 1). Temperature control in the reactor was achieved by circulating cold water through the outer jacket of the UV lamp sleeve. The reactor contents in all batches were continually aerated through a perforated quartz disc at a flow rate of 10 m$\ell\cdot$min^{-1}. Total reaction time in all systems was 60 min. 12 mℓ aliquots of the test solution were withdrawn from the reactor at predetermined intervals and filtered through 0.22 μm syringe filters (Millipore). 10 mℓ of the filtered solution was analysed for residual geosmin in solution after the addition of 3 g of pre-dried NaCl in sealed headspace vials.

Analysis

Progress of geosmin degradation was monitored by GC/MS analysis in a Clarus 600T GC/MS (Perkin Elmer, Connecticut, USA) equipped with a Perkin Elmer Elite – 5MS capillary column (30 m x 0.25 mm ID x 0.5 μm fixed phase) with helium as carrier gas. The GC detectors were bypassed in this method. Sample extraction was achieved online by a Turbo Matrix 40 Headspace Autosampler equipped with a trap. Organics in the sample were extracted by heating at a headspace oven temperature of 80°C for 40 min at a vial pressure of 30 psi (206.84 kPa). The extracts were then desorbed onto the GC column at a pressure of 15 psi (103.42 kPa). The GC oven was programmed at a temperature gradient of 40°C$\cdot$min^{-1}, ramped at 6°C$\cdot$min^{-1} to 150°C and at 15°C$\cdot$min^{-1} from 150°C to 250°C. Geosmin concentration was obtained from calibration curves of standards. Reaction intermediates were identified from samples analysed during the height of activity in the reactors using spectral comparison with those in the NIST chemical spectral database (NIST, Gaithersburg, Maryland, USA).
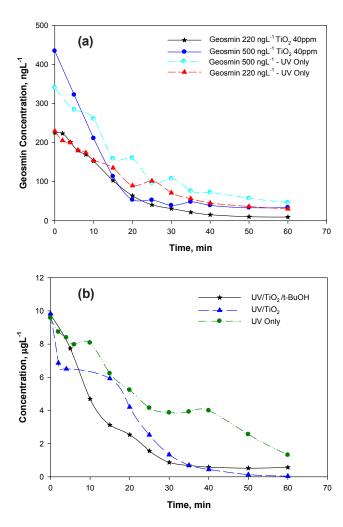
Results and discussion

Geosmin degradation

Firstly, the degradability of geosmin was tested in the range above the human odour detection threshold of 1.3 ng$\cdot\ell^{-1}$. The catalyst concentration tested earlier under similar conditions, 40 mg $TiO_2 \cdot \ell^{-1}$ (Bamuza-Pemu and Chirwa, 2010), was chosen

Table 1
Geosmin degradation efficiency in batches under varying initial concentration

Initial concentration (ng·ℓ⁻¹)	Experimental condition	Final concentration (ng·ℓ⁻¹)	Final removal (after 60 min) %
220	TiO₂/UV	9.8	95.8
220	UV Only	28.8	86.9
500	TiO₂/UV	33.7	92.3
500	UV Only	68.3	86.4
10 000	TiO₂/UV	36.0	99.6
10 000	UV Only	1311	86.3
10 000	TiO₂/UV/t-BuOH[a]	568	94.2

a Experiment with the ·OH scavenger t-BuOH

Figure 2
Degradation profile of geosmin at the initial concentration of (a) 220 and 500 ng·ℓ⁻¹ and (b) 10 µg·ℓ⁻¹

for the current study. Overall removal in the range of 92–95% was observed in the batches spiked with 220 and 500 ng·ℓ⁻¹ and up to 86% in batches spiked with 10 µg·ℓ⁻¹ (Table 1, Figs. 2a, b). The presence of radical scavengers during the photocatalytic degradation had a negative effect resulting in a 6% reduction in the degradation efficiency observed in the 10 µg·ℓ⁻¹ batch (Table 1).

Photolytic degradation kinetics

The reactive component in the presence of UV light was earlier determined to be the hydroxyl radicals (OH) generated from the splitting of water by electromagnetic waves (Schwarzenbach et al., 2003). The rate of reaction of any compound will therefore be dependent on the availability of reactive sites, i.e., a concentration will be reached when the amount of reactant in the system exceeds the amount of hydroxyl radicals (OH) produced, at which point the amount of reactant supplied is at equilibrium with the amount of oxidant. The saturation kinetics can thus be applied in a system with increasing reactant concentration as follows:

$$v = \frac{kC \cdot C_{\bullet OH}}{K_C + C} \tag{1}$$

where:
C = concentration of geosmin (ng·ℓ⁻¹) at time t
$C_{\cdot OH}$ = concentration of hydroxyl radicals (ng·ℓ⁻¹) generated at the given UV light intensity
v = geosmin oxidation rate (ng·ℓ⁻¹min⁻¹)
k = reaction rate coefficient (min⁻¹)
K_C = half velocity concentration of geosmin (ng·ℓ⁻¹)

In the above equation, the multiple of the degradation rate coefficient (k) and the maximum achievable hydroxyl radical concentration ($C_{\cdot OH}$) yields the maximum reaction rate coefficient, $v_{max} = k \times C_{\cdot OH}$ (ng·ℓ⁻¹min⁻¹). In this study, a much lower concentration of geosmin was evaluated in the ng·ℓ⁻¹ range. Under these conditions, geosmin concentration could be much lower than the half-velocity concentration, $K_C \gg C$, such that the group $k \times C_{\cdot OH}/K_C$ becomes constant and Eq. (1) is reduced to the first-order form:

$$v = \left(\frac{k \cdot C_{\bullet OH}}{K_C} \right) \cdot C \tag{2}$$

Equation (2) is evaluated using the experimental data by plotting $\ln(C/C_o)$ versus t and the slope is a constant $k \times C_{\cdot OH}/K_C$ represented by the pseudo-constant k' (min⁻¹). The data from 3 sets of experiments at initial concentrations of 220 ng·ℓ⁻¹, 500 ng·ℓ⁻¹ and 10 ·µg·ℓ⁻¹ was evaluated and the closeness of fit was demonstrated by the high values of the regression coefficient (r^2) obtained (Table 2). The model fitness confirms that the driving factor of photolytic degradation for geosmin is indeed the hydroxyl radical. The results show that the degradation rate coefficient k' was relatively constant regardless of the initial concentration of geosmin used in this range, which further confirms the relevance of the photolytic reaction via hydroxyl radical oxidation as represented by Eqs. (1) and (2) above.

Photolytic reaction with particle surface catalysis

Particles contribute to light attenuation in a water sample, both by light absorption and scattering. Depending on which effect is predominant, the rate of direct photolysis of a dissolved species in a given system may be decreased or enhanced (Schwarzenbach et al., 2003). Experimental observations in the case of titanium dioxide (TiO₂) showed a marked increase in degradation of geosmin (Fig. 2). The slightly enhanced degradation was attributed to the possibility of extra oxidation reactions occurring near or at the solid semiconductor surfaces. Preliminary inspection of degradation rate kinetics in the presence of TiO₂ clearly showed that geosmin degradation in the presence of the TiO₂ particles did not comply with
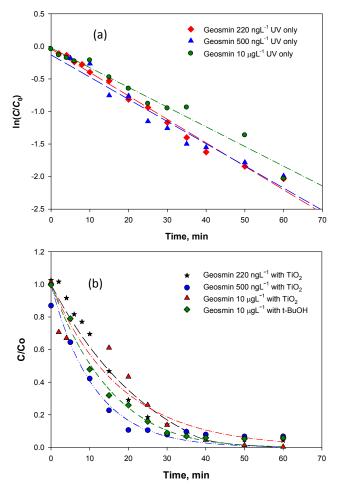
Figure 3
Modelling geosmin degradation rate (a) with UV only showing first-order rate kinetics and (b) with UV and 40 mg·ℓ⁻¹ TiO₂ showing saturation kinetics

sites superseded the rate of conversion at the sites. A concurrent reaction analogous to the Langmuir equation must then occur at the particles as follows:

$$v_s = \frac{k_q \cdot K_q C_s}{1 + K_q C_s} \cdot M_s \tag{3}$$

where:
k_q = maximum specific surface degradation rate coefficient (min⁻¹)
K_q = surface affinity coefficient (ℓ·mg⁻¹)
C_S = concentration at the particle surface (mg·ℓ⁻¹)
M_S = concentration of catalysts in the system (mg·ℓ⁻¹)

If the mass of the catalysis is not changing, then the group of terms $k_q K_q M_S$ will be constant and can be replaced by the pseudo-constant value $k_q' = k_q K_q M_S$ (min⁻¹). The concentration at the surface C_s is a function of the bulk liquid concentration C and is influenced by the diffusion rate coefficient and amount of catalysts in the system. If the two reactions, photolytic degradation and catalytic degradation, occur simultaneously, the system cannot be solved algebraically; thus a numerical solution is achieved using the Computer Program for the Identification and Simulation of Aquatic Systems AQUASIM 2.01 (AQUASIM™, EAWAG, Dübendorf, Switzerland). The fitness of the model is demonstrated by the reasonably good fit (Fig. 3b) with non-linear regression coefficients ranging from 0.95–0.99 (Table 2). The optimum surface affinity coefficient K_q for all batches tested was near constant at K_q = 4.55±0.03 ℓ·mg⁻¹.

Finally, the quenching effect of the scavenger t-BuOH can be evaluated as a direct detractor of the hydroxyl radical ·OH. It should be noted, however, that, in this case, t-BuOH may not discriminate between radicals produced due to photolysis and those produced due to photocatalysis on the TiO₂ particles. In the photocatalytic reaction, the amount of hydroxyl radical produced at the surface of the particles will be directly proportional to the concentration of catalyst. This introduces a second source term for $C_{·OH}$ and the surface reaction can be generalised as shown in Eq. (5). The dimensionless quenching factor F_x is therefore applied to the two predominant reaction terms as follows:

$$v_L = \left(\frac{k \cdot C}{K_C} \right) \cdot \left(C_{·OH} - \frac{C_{x0} - C_x}{F_x} \right) \tag{4}$$

$$v_s = \frac{k_q \cdot C}{1 + K_q C} \cdot \left(C_{·OH} - \frac{C_{x0} - C_x}{F_x} \right) \tag{5}$$

the first-order reaction rate kinetics (data not shown). At the moment, the uncertainty about the amount of ·OH generated affects the reliability of the model. However, the stability of the parameter k' could serve as an indirect indicator of the stability of this parameter.

Since the observed increase in geosmin degradation was, at best, minimal, we assume reaction rate limitation of the overall removal of geosmin associated with the particles. In other words, the rate at which geosmin molecules reach the reaction

Table 2
Geosmin degradation kinetics fitting the photolytic and surface reaction model

Initial concentration (ng·ℓ⁻¹)	Experimental conditions	Degradation rate coefficient k' (min⁻¹)	Surface reaction coefficient k_q' (min⁻¹)	Extinction factor ·OH F_x (ng·ng⁻¹)	Regression coefficient r^2
220	UV only	0.036	--	--	0.987
500	UV only	0.034	--	--	0.947
10 000	UV only	0.030	--	--	0.970
220	TiO₂/UV	0.021	0.099	--	0.892
500	TiO₂/UV	0.036	0.090	--	0.964
10 000	TiO₂/UV	0.055	0.027	--	0.937
10 000	TiO₂/ UV/t-BuOH[a]	0.038	0.055	2.554	0.982

[a] Experiment with the ·OH scavenger t-BuOH

where:

v_L = rate of degradation due to photolysis (ng·ℓ$^{-1}$·min^{-1})

v_s = rate of degradation due to particle surface reaction (ng·ℓ$^{-1}$min^{-1})

k = photolytic rate coefficient via hydroxyl radical (min^{-1})

k_q = specific surface reaction rate coefficient (min^{-1})

C_0 = geosmin concentration (ng·ℓ$^{-1}$) in the batch at time zero

F_x = the $C_{·OH}$ quenching factor (ng ·OH extinguised per ng t-BuOH oxidised)

Contradictory results were obtained regarding the effect of t-BuOH in the system. Although results show inhibition of the reaction in the final stages of the experiment, the initial reaction was faster than the reaction in batches with TiO$_2$ only (Fig. 3b). This is also reflected in the increased specific reaction coefficients in the solution and the surface (Table 2). However, the extent of removal is affected by the quenching factor in the final stages. We expect that the effect of the scavenging activity could be more defined at higher concentrations of the scavenger.

Degradation pathways and intermediates formed

Intermediate products formed during the photocatalytic degradation of geosmin were studied to obtain a better understanding of the pathway during photocatalysis and to ascertain that intermediates formed during the process are not environmental threats. Earlier studies with geosmin at environmentally significant levels resulted in total mineralisation of geosmin and degradation intermediates (Chirwa and Bamuza-Pemu, 2010). In this study, a 10 μg·ℓ$^{-1}$ concentration of geosmin was used in the degradation experiments to avoid the total elimination zone and to study the transitional compounds before mineralisation to CO$_2$ and H$_2$O. Three possible reactive pathways for the degradation of geosmin in solution can be identified, including:

- oxidation by hydroxyl radicals;
- oxidation by reactive holes on the surface of the catalyst; and
- direct photolytic cleavage by exposure to UV radiation.

Control experiments with the catalyst in the absence of UV radiation gave no appreciable reduction in geosmin concentration, indicating that reduction in geosmin concentration is due to the suggested reactive pathways and no significant losses from evaporation and other unidentified sources occurred.

Geosmin is a bicyclic` tertiary alcohol (Fig. 4) with mainly single covalently bonded sp^3–sp^3 (C–C) bonds with bond energies of 83–85 kcal mol^{-1}, sp^3–O (C–O) bond with bond energies of 85–91 kcal mol^{-1}, sp^3–H (C–H) bond with bond energies of 96–99 kcal·mol^{-1} and an O–H bond with bond energies 110–111 kcal mol^{-1} (Smith and March, 2006). UV light with λ_{max} at 365 nm has energy of 78.28 kcal·mol^{-1}, which is of
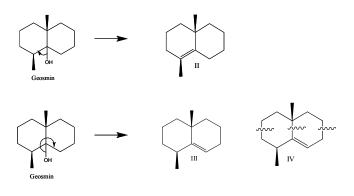

Figure 4

Structure of geosmin and possible dehydration products II and III

the same order of magnitude and comparable with bond energies in geosmin. There exists the possibility of photolytic bond cleavage at 365 nm, at the C–O and C–C bonds. Cleavage of the C–O bonds could lead to a more stable tertiary carbocation. This is followed by an adjacent hydrogen abstraction leading to two possible dehydration products – (1*S*,4a*R*)-1,4a-dimethyl-1,2,3,4,4a,5,6,7-octahydronaphthalene (Product II) and (R)-4a,8-dimethyl-1,2,3,4,4a,5,6,7-octahydronaphthalene (Product III), with the elimination of water.

Bond fission is also possible at all C–C bond cites with subsequent opening of the ring structure of both geosmin and the dehydration products II and III, and skeletal rearrangement leading to the formation of a collection of acyclic saturated and unsaturated compounds. GC/MS data for geosmin and some of the identified intermediate compounds are presented in Table 3. Degradation intermediates identified from GC/MS analysis include 3,5-dimethlyhex-1-ene(V), which would most likely be a product of ring fission at positions indicated in Fig. 5 (Product IV). Other intermediate products identified include 2,4-dimethlypentan-3-one (VI), 2-methylethyl-propanoate (VII), 2-heptanal (VIII) (Fig. 5).

Products from the direct dehydration of geosmin (dehydration products II and III) were not identified during GC/MS analysis of intermediates. Geosmin has 10 C–C bonds, while dehydration products II and III each contain 9 C–C bonds with the same bond energies; bond dissociation can occur at any of the 9 C–C bond cites each resulting in decyclization. This suggests that bond fission, resulting in ring opening of geosmin cyclic structure and that of dehydration/dehydrogenation products, occurs rapidly and simultaneously at all C–C bonds within the cyclic structure during photocatalysis. The dehydration products are believed to be transient intermediate species due to the various possible points of bond fission and ring opening. Intermediates VII and VIII are most likely ring opening products of compound IX, which were not identified in the present study, but were identified as an intermediate product of

Chemical formula	Compound No. in Fig. 5	Retention time (min)	Match probability	Major ions for identification
C12H22O(geosmin)		24.98	Standard	112,41,55,111,125,43,97
C8H16	V	15.64	824	41,31,55,57,70,83
C7H14O	VI	24.06	759	43,71,56,55,41,39
C6H12O2	VII	24.06	766	43,71,55,41,39
C7H12O	VIII	15.64	751	41,31,55,57,70,83

Table 3
GC/MS data of geosmin and some identified intermediate compounds

Figure 5
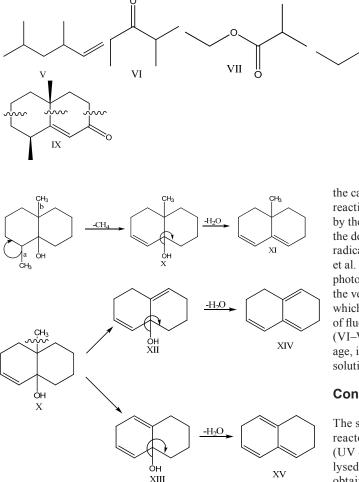*Structures of some identified degradation products*

Figure 6
Structure of geosmin and possible products from the elimination of methane

microbial degradation of geosmin by Saito et al. (1999).

Cleavage of the C—C bonds of the terminal methyl group (a) with the elimination of methane would produce a transient intermediate product (X); further cleavage of methyl group (b) from Product X yields intermediate products XII and XIII (Fig. 6).

Elimination of water from intermediate products X, XII and XIII, which, on decyclisation from C—C bond cleavage, would account for the acyclic hydrocarbons produced. The intermediate products identified during the partial degradation experiment are not found on the US EPA priority pollutants list (US EPA, 2011). However, their existence has important implications regarding the formation of potentially carcinogenic trihalomethanes (THMs) and haloacetic acids (HAAs) during chlorine disinfection.

Predominant pathway of degradation

Degradation of organic compounds by photocatalysis is often attributed to reaction with highly reactive hydroxyl radicals generated in solution (Lawton et al., 2003); the current study indicates that there is synergic contribution of the three possible reactive paths leading to the rapid degradation of geosmin in solution. This can be attributed to the significant level of degradation achieved with UV radiation alone in the absence of

the catalyst. However, reaction rate constants obtained for the reactions where hydroxyl radicals in solution were quenched by the introduction of tertiary butanol (Table 2) indicate that the dominant reactive pathway is via oxidation by hydroxyl radicals in solution. This is consistent with findings by Trans et al. (2009) in their study on the effect of ionic species on the photocatalytic degradation efficiency of geosmin. This is due to the very high oxidative potential of hydroxyl radicals (2.8 V), which is higher than most other oxidants, with the exception of fluorine. The presence of oxygenated degradation products (VI–VII) (Fig. 5), rather than only products from bond cleavage, is also an indication of the presence of oxidative species in solution.

Conclusion

The study shows that geosmin degradation in the photoreactor followed first-order kinetics for photolytic reaction (UV only) and mixed-order kinetics for the reaction catalysed by TiO_2 semiconductor particles. Intermediate products obtained from rapid photolytic/photocatalytic degradation of geosmin in solution were also identified. The results show that geosmin undergoes rapid ring opening and subsequent bond cleavage at multiple sites to produce acyclic saturated and unsaturated compounds including some alkanones and esters. Complete mineralisation was achieved in earlier studies in batches operated at low geosmin concentrations. Complete mineralisation of intermediates accumulated at higher initial geosmin concentration could require longer reaction times or additional stages if used in a continuous flow process. The kinetic analysis results suggest the hydroxyl radical (·OH) as the critical reactant in the system. Thus, engineering of the photolytic/photocatalytic system could focus on maximising oxidative potential by enhancing the processes responsible for generating ·OH.

Acknowledgement

References

BAMUZA-PEMU EE and CHIRWA EMN (2010) Photocatalytic degradation of taste and odour causing compounds in natural water sources. *Chem. Eng. Trans.* **23** 387–392.

CANE DE, HE X, KOBAYASHI S, ŌMURA S, IKEDA H (2006) Geosmin biosynthesis in *Streptomyces avermitilis*. Molecular cloning, expression, and mechanistic study of the germacradienol/geosmin synthase. *J. Antibiot.* **59** (8) 471–479.

CHIRWA EMN and BAMUZA-PEMU EE (2010) Investigation of photocatalysis as an alternative to other advanced oxidation processes for the treatment of filter backwash water. WRC Report No. 1717/1/10. Water Research Commission, Pretoria.

GRIFFINI O, BAO ML, BURRINI D, SANTIANNI D, BARBIERI C and PANTANI F (1999) Removal of pesticides during drinking water process at Florence water supply, Italy. *Aqua* **48** (5) 177–185.

HO L and NEWCOMBE G (2010) Granular activated carbon adsorption of 2-methylisoborneol 374 (MIB): pilot- and laboratory- scale evaluations. *J. Environ. Eng.* **136** (9) 965–974.

HO L, NEWCOMBE G and CROUÉ J (2002) Influence of the character of NOM on the ozonation of MIB and geosmin. *Water Res.* **36** (3) 511–518.

LAWTON LA, ROBERTSON PKJ, ROBERTSON RF and BRUCE FG (2003) The destruction of 2-methylisoborneol and geosmin using titanium dioxide photocatalysis. *Appl. Catal. B: Environ.* **44** (1) 9–13.

LLOYD SW, LEA JM, ZIMBA PV and GRIMM CC (1998) Rapid analysis of geosmin and 2-methylisoborneol in water using solid phase micro extraction procedures. *Water Res.* **32** (7) 2140–2146.

NERENBERG R, RITTMANN BE and SOUCIE WJ (2000) Ozone/ biofiltration for removing MIB 404 and geosim. *J. Am. Water Works Assoc.* **92** (12) 85–95.

PETER A and VON GUNTEN U (2007) Oxidation kinetics of selected taste and odor compounds during ozonation of drinking water. *Environ. Sci. Technol.* **41** 626–631.

PHAM TT, NGUYEN VA and VAN DER BRUGGEN B (2012) Evaluation of two low cost – high performance adsorbent materials in the waste-to-product approach for the removal of pesticides from drinking water. *Clean Air Soil Water* **40** (3) 246–253.

SAITO A, TOKUYAMA T, TANAKA A, ORITANI T and FUCHI-GAMI K (1999) Microbiological degradation of (-)-geosmin. *Water Res.* **33** (13) 3033–3036.

SCHWARZENBACH RP, GSCHWEND PM and IMBODEN DM (2003) Environmental Organic Chemistry, John Wiley & Sons Ltd., London.

SMITH MB and MARCH J (2006) *March's Advanced Organic Chemistry: Reactions, Mechanisms, and Structure.* Wiley, New York. 2357 pp.

SONG W and O'SHEA KE (2007) Ultrasonically induced degradation of 2-methylisoborneol and geosmin. *Water Res.* **41** (12) 2672–2678.

TRAN H, EVANS GM, Yan Y and NGUYEN AV (2009) Photocatalytic removal of taste and odour compounds for drinking water treatment. *Water Sci. Technol. Water Supply* **9** (5) 477–483.

TRAN H, EVANS GM, Yan Y and NGUYEN AV (2008) Photocatalytic removal of geosmin and MIB and its potential applications for drinking water treatment. *Proc. Environ 08*, 5–7 May 2008, Melbourne, Australia.

YOUNG WF, HORTH H, CRANE R, OGDEN T and ARNOTT M (1996) Taste and odour threshold concentrations of potential potable water contaminants. *Water Res.* **30** (2) 331–340.

US EPA (UNITED STATED ENVIRONMENTAL PROTECTION AGENCY) (2011) List of priority pollutants. URL: http://water.gov/ scitech/methods/cwa/pollutants (Accessed 24 May 2012).

WATSON SB, RIDAL J, ZAITLIN B and LO A (2003) Odours from pulp mill effluent treatment ponds: the origin of significant levels of geosmin and 2-methylisoborneol (MIB). *Chemosphere* **51** (8) 765–773.